HHS Public Access

Author manuscript

Brain Res. Author manuscript; available in PMC 2016 April 24.

Published in final edited form as:

Brain Res. 2015 April 24; 1605: 22–30. doi:10.1016/j.brainres.2015.02.012.

Auditory nerve synapses persist in ventral cochlear nucleus long after loss of acoustic input in mice with early-onset progressive hearing loss

Brian McGuire[a], **Benjamin Fiorillo**[a], **David K. Ryugo**[b,c], and **Amanda M. Lauer**[a]

[a] Center for Hearing and Balance and Department of Otolaryngology-HNS, Johns Hopkins University, Baltimore, MD, 21205 USA

[b] Hearing Research Unit, Garvan Institute of Medical Research, Darlinghurst, New South Wales, 2010 Australia

[c] School of Medical Sciences, University of New South Wales, Kensington, New South Wales, 2052, Australia

Abstract

Perceptual performance in persons with hearing loss, especially those using devices to restore hearing, is not fully predicted by traditional audiometric measurements designed to evaluate the status of peripheral function. The integrity of auditory brainstem synapses may vary with different forms of hearing loss, and differential effects on the auditory nerve-brain interface may have particularly profound consequences for the transfer of sound from ear to brain. Loss of auditory nerve synapses in ventral cochlear nucleus (VCN) has been reported after acoustic trauma, ablation of the organ of Corti, and administration of ototoxic compounds. The effects of gradually acquired forms deafness on these synapses are less well understood. We investigated VCN gross morphology and auditory nerve synapse integrity in DBA/2J mice with early-onset progressive sensorineural hearing loss. Hearing status was confirmed using auditory brainstem response audiometry and acoustic startle responses. We found no change in VCN volume, number of macroneurons, or number of VGLUT1-positive auditory nerve terminals between young adult and older, deaf DBA/2J. Cell-type specific analysis revealed no difference in the number of VGLUT1 puncta contacting bushy and multipolar cell body profiles, but the terminals were smaller in deaf DBA/2J mice. Transmission electron microscopy confirmed the presence of numerous healthy, vesicle-filled auditory nerve synapses in older, deaf DBA/2J mice. The present results suggest that synapses can be preserved over a relatively long time-course in gradually acquired deafness. Elucidating the mechanisms supporting survival of central auditory nerve synapses in models of acquired deafness may reveal new opportunities for therapeutic intervention.

Corresponding author: Amanda M. Lauer, 515 Traylor Building, 720 Rutland Ave., Baltimore, MD 21205 USA. 1-443-287-6336. alauer2@jhmi.edu.

Keywords

ventral cochlear nucleus; auditory nerve; endbulb; hearing loss; deafness

1. Introduction

Peripheral damage patterns and audibility cannot fully account for performance on complex auditory processing tasks or success with hearing devices. For instance, postlingually deafened patients who receive cochlear implants as adults can show speech discrimination and recognition scores of 0 to 100% (Green et al., 2007; Lazard et al., 2010). Central auditory system factors such as deafness-related synaptic alterations, cortical and subcortical reorganization, and capacity for plasticity likely play a critical role in determining outcomes in hearing device recipients. Studies have demonstrated loss of auditory nerve synapses in the ventral cochlear nucleus (VCN) after acoustic overexposure (Kim et al., 2004), surgical destruction of the cochlea (Fyk-Kolodziej et al., 2011; Gentschev and Sotelo 1973), and application of ototoxic substances (Yuan et al., 2014; Zeng et al., 2009a), but the effects of other forms of acquired deafness on these synapses are unclear.

Mouse models provide an efficient means of investigating the effects of different forms of acquired hearing loss on the central auditory system including hereditary and environmental determinants of synaptic integrity. The DBA/2J mouse is one such model in which the genetic contributions to accelerated age-related hearing loss (Johnson et al., 2008; Noben-Trauth et al., 2003; Shin et al., 2010; Someya et al., 2007), and the effects of manipulations to the acoustic environment (Turner and Willott 1998; Willott et al., 2005) have been well characterized. Hearing loss in DBA/2J mice begins at high frequencies around the time of weaning (3-4 weeks) and becomes severe at all but the lowest frequencies by about 4 months of age (Erway et al., 1993; Mikuriya et al., 2008; Someya et al., 2007; Xie and Manis 2013). The hereditary hearing loss is related to a mutation of cadherin 23, a transmembrane protein involved in cell adhesion (Noben-Trauth et al., 2003), and a variant of fascin-2, a developmentally regulated actin crosslinker in hair-cell stereocilia (Shin et al., 2010).

The DBA/2J cochlea initially contains more cochlear hair cells than other inbred strains (Ding et al., 2001). Progressive base-to-apex damage to hair cells in the base of the cochlea occurs within the first six months of age in this strain (Shin et al., 2010; Someya et al., 2007). Spiral ganglion neurons (SGN) are almost completely lost from the base by 6-8 months of age, with partial SGN loss also occurring in apical regions (Mikuriya et al., 2008; Someya et al., 2007; Willott and Erway 1998).

Transmission at auditory nerve endbulb synapses in anteroventral cochlear nucleus (AVCN) is altered in young adult DBA/2J mice (Wang and Manis 2005; Wang and Manis 2006). One and a half to two month old DBA/2J mice show slower and smaller mEPSCs, reduced release probability, higher action potential firing thresholds, larger after-hyperpolerizations, reduced entrainment during long stimulus trains, and shorter spike latencies in high frequency regions compared to younger DBA/2Js (Wang and Manis 2005; Wang and Manis

2006). These mice also show abnormal neural responses in the inferior colliculus and cochlear nucleus in young adulthood (Willott 1981).

We investigated the effects of early-onset progressive hearing loss on the structural integrity of central auditory nerve synapses in deaf DBA/2J mice. We hypothesized that deaf DBA/2J mice would show a reduced complement of auditory nerve synapses in VCN compared to young hearing DBA/2J mice. Surprisingly, we found that auditory nerve synapses in VCN survived in deaf DBA/2J mice, in contrast to what has been described for other forms of acquired deafness.

2. Results

2.1 Hearing screening

2.1.1 Auditory brainstem responses (ABRs)—Individual ABR thresholds for DBA/2J mice ages 1 to 7 months are plotted in Figure 1. Average thresholds from 4 normal-hearing 2-month old mice of the CBA/CaJ strain are shown for comparison. ABR thresholds were elevated for frequencies above 12kHz in DBA/2J mice compared to CBA/CaJ mice, even at 1-2 months of age. Thresholds rapidly increased with age in DBA/2J mice, and the mice were almost completely non-responsive to all but the lowest frequencies by 5 months. Examples of ABR waveforms from a young hearing DBA/2J and an older deaf DBA/2J are shown in Figure 1 B. No synchronous response can be detected by 7 months.

2.1.2 Acoustic startle responses (ASRs)—The ASR was measured for a range of startle-eliciting stimulus intensities in quiet and background noise as shown in Figure 2. ASR amplitude was rarely above background movement levels for four 1-2 month old DBA/2J mice (A, B), even for very loud (100-110 dB SPL) stimuli. No ASR enhancement was observed in the presence of background noise. In contrast, 1-2 month old CBA/CaJ mice (n=7) showed clearly observable ASRs to startle-eliciting stimuli that were presented at 90 dB SPL and greater (C, D). The typical ASR enhancement in noise (Ison 2001) was observed in CBA/CaJ mice. Pilot studies revealed a complete absence of the ASR in DBA/2J mice older than 2 months, so the mice used in the present study were not tested behaviorally at older ages.

2.2 Histological analysis

2.2.1 Stereological analysis—As shown in Figure 3 A, VCN volume estimated using the Cavalieri probe was similar in 1-2 month old (n=6 VCNs from 3 animals) and 9-10 month old (n=5 VCNs from 3 animals) DBA/2J mice ($p=0.380$). Similarly, the number of macroneurons (≥10 microns) in VCN magnocellular core was not significantly different in 1-2 month (n=4 VCNs from 3 mice) compared to 9-10 month (n=4 VCNs from 3 mice) DBA/2J mice ($p=0.70$; Figure 3 B). There was also no significant difference in the number of VGLUT1-positive puncta in the VCNs of 1-2 month (n=3 VCNs from 3 mice) and 9-10 month (n=3 VCNs from 3 mice) DBA/2J mice ($p=0.33$; Figure 3 C).

2.2.2 Cell-type specific analysis—Numerous VGLUT1-positive puncta were observed contacting neurons in VCN core (Figure 4). No qualitative differences in staining patterns

between young and old DBA/2J mice were observed. Bushy cell (p=0.50) and multipolar cell (p=0.11) cross sectional area was not significantly different in 1-2 month and 9-10 month DBA/2J mice. The number of puncta per 10 microns of cell body perimeter was similar in young and older DBA/2Js for both bushy (p=0.57) and multipolar cells (p=0.94). Cross-sectional area of VGLUT1 puncta contacting bushy cells (p<0.0001) and multipolar cells (p<0.0001) was larger in 1-2 month old DBA/2Js compared to 9-10 month old DBA/2Js. Averages and standard deviations are summarized in Table 1.

2.2.3 Transmission electron microscopic (TEM) verification of auditory nerve synapse integrity—The status of auditory nerve synapses in VCN was verified through TEM analysis. The ultrastructure of bushy cells and their endbulb synapses has been characterized in several strains of mice (Lauer et al., 2013; Lee et al., 2003) and, thus, this type of synapse was selected for analysis. Bushy cells from both hearing and deaf DBA/2J mice had round or ovoid cell bodies with round nuclei, pale cytoplasm, and numerous strands of rough endoplasmic reticulum with associated ribosomal rosettes. No substantial ultrastructural differences were observed between bushy cells from hearing and deaf DBA/2J mice. Numerous axosomatic endbulb profiles containing clear, large round synaptic vesicles were observed in both groups of mice. Endbulb profiles from young DBA/2J mice (Figure 5 A) resembled those described in normal-hearing CBA/CaJ mice (Lauer et al. 2013), characterized by the presence of numerous large round synaptic vesicles; curved, asymmetric postsynaptic densities (psd); extended extracellular spaces, and layered glial sheaths (glia). Deaf, ~7-8 month old DBA mice showed endbulb profiles that appeared predominantly normal (Figure 5 B). Occasionally, long, flat psd profiles reminiscent of endbulbs in congenitally deaf animals were observed. Retracting or missing synapses were not observed.

3. Discussion

We have shown that auditory nerve synapses survive in VCN despite profound deafness in the DBA/2J mouse model of early-onset progressive hearing loss. The results of the present study are surprising in light of earlier studies showing extensive degeneration of auditory nerve synapses in VCN in animals with acute induced hearing loss. The data suggest that the manner in which deafness is produced determines which signaling pathways get activated that result in damage to central auditory synapses. That is, pharmacologic, traumatic, or inherited, progressive forms of hearing loss can yield different modes of degeneration and/or elicit different trophic signals. The different signaling cascades may up- or down-regulate variable cell death pathways that allow for neural preservation to a different degree than, for example, in acute trauma to the cochlea.

3.1 Hearing status

The DBA/2J mice tested in the present study showed predictable early-onset progressive hearing loss beginning around 2 to 3 months of age. Behavioral responses to sounds were diminished in DBA/2J mice even at 1-2 months of age compared to normal-hearing CBA/CaJ mice. Facilitation of the acoustic startle response by background noise was absent in young adult DBA/2J mice, indicating the possibility of abnormal central processing of

sounds at an age when the auditory periphery remains relatively intact. Despite the loss of sound-evoked activity, auditory nerve synapses remained relatively unchanged even after months of deafness as discussed in detail below.

3.2 VCN integrity and auditory nerve synapse survival

We found no difference in total VCN volume or in the number of macroneurons between young hearing and older deaf DBA/2J mice. Further analysis revealed no difference in cell body cross-sectional area in these two groups of mice. These results differ from a previous study that reported slight decreases in the number of neurons and anterior VCN volume in DBA/2J mice (Willott et al., 2005). We attribute the differences to different quantification procedures. The previous study used quantification methods that are subject to significant sampling biases, whereas our stereological quantification procedures avoid those biases. Numerous VGLUT1-positive puncta representing auditory nerve terminals were observed throughout the VCN of both young hearing and older deaf DBA/2J mice. Most puncta contacted bushy, stellate, and octopus cell bodies, but puncta were also observed in the neuropil, presumably contacting dendrites. The total number of VGLUT1-positive auditory nerve puncta observed in VCN core was unchanged between young hearing and older deaf DBA/2J mice. Similarly, the number of puncta contacting bushy and multipolar cell body profiles was not different.

The only significant difference between young hearing and older deaf mice that was identified was a reduction in puncta cross-sectional area. This result could be interpreted as reflecting ending shrinkage or reduced VGLUT1 activity within auditory nerve synapses. TEM analysis indicated that the synapses were healthy in deaf DBA/2J mice. The presence of numerous synaptic vesicles in close proximity to presynaptic and postsynaptic membrane specializations argues that the synapses remain active. A proliferation of vacuoles was not observed in DBA/2J auditory nerve terminals, and obvious signs of degenerated or missing profiles was not evident. Thus, we infer that auditory nerve terminals survive in the VCN of deaf DBA/2J mice at least until 9-10 months of age. Furthermore, the presence of synaptic vesicles and healthy mitochondria indicate that these synapses are capable of being activated. The survival of central auditory nerve synapses reported in the present study is in stark contrast to what has been reported for mechanical, ototoxic, or noise-induced trauma to the cochlea (Gentschev and Sotelo 1973; Kim et al., 2004; Yuan et al., 2014; Zeng et al., 2009a). It will be critical in future studies to determine why some causes of hearing loss produce a loss of central synapses whereas others do not.

3.3 Factors affecting auditory nerve synapse survival

There are several factors that could extend the survival of central auditory nerve synapses in DBA/2J mice. Spontaneous activity in auditory nerve fibers may persist in the absence of acoustic stimulation. Acute cochlear insult alters spontaneous discharge rates in the auditory nerve (Furman et al., 2013; Liberman and Kiang 1978; Liberman and Dodds 1984), but C57BL6 mice with progressive, hereditary hearing loss appear to have normal spontaneous activity at the onset of hearing loss (Lang et al., 2002; Taberner and Liberman 2005). It is unknown how long the spontaneous activity persists after hearing loss develops in DBA/2J mice.

Changes in innervation by cholinergic efferent neurons may also support survival of central auditory nerve synapses in DBA/2J mice in the absence of acoustic stimulation. Sprouting of cholinergic fibers occurs in VCN following acute noise trauma and cochlear ablation (Hildebrandt et al., 2011; Kraus et al., 2011; Meidinger et al., 2006). This cholinergic plasticity has been proposed as a mechanism to protect against the development of tinnitus after cochlear injury (Kraus et al. 2011). Plasticity of peripheral olivocochlear efferent innervation occurs in mice with hereditary progressive hearing loss (Lauer et al., 2012). It is possible that similar olivocochlear efferent sprouting also occurs when peripheral input is diminished in progressive forms of hearing loss.

Activation of cholinergic receptors in the hippocampus increases expression of neurotrophins, which have been shown to increase cholinergic activity (Knipper et al., 1994a; Knipper et al., 1994b). Neurotrophins support survival of spiral ganglion neurons after inner hair cell loss (Miller et al., 1997), and neurotrophin expression increases in the cochlear nucleus after acute cochlear damage (Mulders et al., 2014; Suneja et al., 2005). Thus, increased innervation by cholinergic efferent neurons and enhanced neurotrophic signaling may work synergistically to promote survival of central auditory synapses.

Though our analysis did not reveal signs of synaptic degeneration in 9-10 month old DBA/2Js, we cannot rule out the possibility that central auditory nerve synapses degenerate at later ages and with longer periods of deafness. Our study also cannot rule out the possibility of more subtle changes that are not detectible using our techniques. For instance, the form or complexity of endbulbs of Held could be altered in localized frequency regions or in a small subset of neurons. Additionally, changes to the number of inhibitory or non-primary excitatory (from sources other than the auditory nerve) inputs may occur in deaf DBA/2J mice.

3.4 Summary and conclusions

Auditory nerve synapses are preserved at least until 9-10 months of age in deaf DBA/2J mice. This result is in contrast with what occurs in other forms of acquired permanent hearing loss within about 1 month of the cochlear insult. Survival of central auditory nerve synapses will likely affect the outcomes of hearing-impaired patients receiving treatments designed to restore or replace cochlear function, and the present results suggest that synapses can be preserved in some forms of acquired deafness. Elucidating the mechanisms that promote survival of central auditory nerve synapses in acquired deafness may provide new opportunities for therapeutic intervention.

4. Experimental Procedures

4.1 Subjects

Male and female DBA/2J mice (JAX stock #000671) and normal-hearing ages 1-10 months were used as subjects. A total of 36 DBA/2J mice were used in the study. For comparison, 7 normal-hearing male CBA/CaJ mice (JAX stock #000654) were used in the hearing screening experiments. Animals were housed in filter top shoebox cages in a quiet, low-traffic room (Lauer et al., 2009). All procedures were approved and performed in

accordance with the Guide for the Care and Use of Laboratory Animals, Johns Hopkins University Animal Care and Use Committee, and the Garvan/University of New South Wales Animal Ethics Committee.

4.2 Hearing Screening

4.2.1 Auditory brainstem responses (ABRs)—The DBA/2J strain was re-derived around 2002 according to the strain information provided by the Jackson Laboratory, so we conducted functional assessments of brainstem responses and behavioral responses to sound to verify the hearing loss phenotype. Procedures for collecting ABRs were similar to those previously described in our lab (Lauer and May 2011; Lina and Lauer 2013). Mice were anesthetized with 100mg/kg ketamine and 20mg/kg xylazine (i. p.) and placed inside a small sound-attenuating chamber 30 cm from a speaker. The animals' core temperature was maintained at 37°C ±1°. ABRs were differentially recorded from the scalp using subcutaneous platinum needle electrodes (G.R.A.S.) placed over the left bulla and at the vertex of the skull. A ground electrode was inserted into the leg muscle. Responses were amplified (ISO-80, World Precision Instruments) and bandpass filtered from 30 to 3,000 Hz (Krohn-Hite). Stimulus generation and ABR measurements were controlled and collected using Tucker Davis technologies programming modules, custom Matlab-based software, and a PC. Responses were averaged over 300 stimulus presentations to improve the signal-to-noise ratio. Thresholds and suprathreshold responses to clicks and 5 ms tones (4, 8, 12, 16, 24 kHz) played at 10/s or 20/s were measured by presenting a descending series of stimulus levels until no response could be discerned from the noise. Threshold was defined as the sound level at which the ABR magnitude was 2 standard deviations above the average baseline noise level. When no response was observed even at the loudest stimulus intensity presented, a nominal threshold value of 100 dB was entered in order to facilitate data representation.

4.2.2 Acoustic startle reflex (ASR)—Reactions to startle-eliciting sounds were measured in 4 DBA/2J mice and 7 CBA/CaJ mice. The mouse was placed inside a small testing cage (4 ½" × 1 ½" × 1 1/8") constructed of Delrin and wire mesh. The cage was placed on top of a piezoelectric disk mounted in a platform made of Delrin and placed inside a small sound-attenuating chamber (IAC Acoustics) lined with acoustic foam (Sonex) to control reflections. The outputs from the piezoelectric disks were amplified with a custom-built amplifier, sampled digitally, and recorded over a 100 ms window following the presentation of a startle-eliciting stimulus. Two Radio Shack supertweeter speakers were placed 10 cm in front of the cage. Experimental parameters and stimulus presentation were controlled using a PC, Tucker Davis Technologies hardware, and custom Matlab-based software. Prior to the initiation of the experiment, the mouse was given a 3-5 min. acclimation period. After this period, stimulus presentation was initiated. Startle-eliciting stimuli consisted of 20-ms broadband noise bursts (4,000-40,000 Hz) presented at 70, 80, 90, 100, and 110 dB (Z) SPL presented either in quiet or in the presence of continuous 60 dB (Z) broadband background noise. Only one background condition (quiet or noise) was tested within a session, and the order of background conditions was randomized. Stimulus levels were presented in a pseudo-randomized order within blocks of trials. A total of 10 trials were tested for each level. The intertrial interval varied between 10 to 20 ms. Trials

were delayed if the animal's movement exceeded baseline "at rest" levels in the 5 ms period prior to the trial.

4.3 Histology, Stereological Analysis, and Transmission Electron Microscopy (TEM)

4.3.1 General tissue preparation—Tissue processing procedures were similar to those reported previously by our lab (Lauer et al., 2013). Mice were deeply anesthetized with Nembutal (50mg/cc i. p.) and perfused intracardially with sodium nitrite followed by a 4% paraformaldehyde or 2% paraformaldehyde, 2% glutaraldehyde fixative solution. Bone was removed over the cerebellum, and the specimens were post-fixed overnight in the perfusion solution. The following day, brains were dissected from the skull, blocked, and embedded in gelalbumin. Coronal sections were cut at a thickness of 50 microns with a vibrating microtome and collected in cold 0.12M PBS solution. Sections were either processed for immunohistochemistry or TEM as described below or mounted onto glass slides, stained with cresyl violet, dehydrated, and cover-slipped.

4.3.2 Immunohistochemistry—Sections were labeled with antibodies against vesicular glutamate transporter 1 (VGLUT1). VGLUT1 is a marker for auditory nerve terminals in the cochlear nucleus (Gómez-Nieto and Rubio 2009; Lauer et al., 2013; Zeng et al., 2009b).

Immunohistochemistry was performed on free-floating sections by blocking with 1% normal goat serum for 1 hour, and incubating overnight @ 4°C in 1:1000 rabbit anti-VGLUT1 (Invitrogen #48-2400). The following day, tissue was incubated in 1:200 goat anti-rabbit secondary (Vector Labs #BA-1000) for 1 hour. The biotinylated antibodies were then detected utilizing the Vectastain Elite ABC Kit (Vector Laboratories #PK-6100) and stained with nickel diaminobenzidine. Negative controls (processed with buffer only during primary antibody incubation) were run on at least one section per brain. Positive controls for VGLUT1 reactivity were cerebellum and cortex. Some sections were counterstained using cresyl violet to allow visualization of target neurons including the principal cell types of VCN: bushy, stellate, and octopus cells. All sections were mounted on glass slides, dehydrated, and cover-slipped.

4.3.3 Stereological analysis—Nucleus volume, number of large neurons (greater than or equal to 10 microns), and the number of VGLUT1-positive puncta VCN core (excluding granule cell area) were quantified using StereoInvestigator software (MBF Biosciences). Measurements were completed by an observer who was blind to the functional hearing status of the animals. A subset of measurements was repeated by a second observer to confirm their accuracy. Parameters were determined based on pilot experiments. Every other section through VCN was analyzed, making the section sampling fraction (ssf) ½.

Area measurements were taken with the Cavalieri probe. The entire profile of VCN excluding the granule cell areas was traced in every other section. When utilizing the Cavalieri probe to estimate the area of a region, a randomly placed 10μm grid was used. This parameter satisfied Gunderson's rule that a total coefficient of error of less than 0.05 is adequate for an accurate quantitative estimate (Gunderson, 1987). Regions of interest were traced at 10x magnification, the grid was placed over those regions, and the software automatically calculated the number of grid points within the regions. To calculate the

estimated volume, the software multiplied the number of points quantified by their associated area or grid size squared to obtain the total sectional area. Multiplying the sectional area by the thickness factor (mean section cut thickness * interval of the sections measured). Student's t-tests were calculated to identify statistically significant differences in stereological estimates of volume.

The optical fractionator probe was used to quantify the total number of macroneurons within the VCN core. A counting frame of 75 × 75 μm and a grid size of 140 × 190 μm were used to generate approximately 10 sampling sites on average per tissue section. The area sampling fraction (asf) was 0.211. A dissector height of 10 μm with no guard zone was used to further the un-bias quantitative analysis. A contour region was traced around the VCN using a 10x objective. Stereological procedures using the optical fractionator probe have been described in detail elsewhere (Schettino and Lauer 2013). The sampling grid was randomly positioned over the section, and the software positioned counting frames automatically. At each counting site, the observer measured the section thickness and placed markers on items falling within the counting frame. The software automatically computed neuron counts based on the sampling fractions, section thickness, and number of markers observed. Student's t-tests were calculated to identify statistically significant differences in stereological estimates of large neuron number.

The optical fractionator probe was also used to quantify the number of VGLUT1-positive puncta within VCN core. The counting frame size was 12μm × 12μm and the grid size was 80 × 100 μm. The asf was therefore 0.018. Counting of objects proceeded as described above. Student's t-tests were calculated to identify statistically significant differences in stereological estimates of VGLUT1-positive puncta.

4.3.4 Cell-type specific analysis—Cross sections of cells identified as bushy cells or multipolar cells and the VGLUT1-positive puncta contacting the cell bodies from three 1-2 month old and three 9-10 month old were photographed using a Nikon light microscope fitted with a 100x oil objective and a Jenoptik camera. Cell types were identified using previously published criteria for mice (Lauer et al., 2013). Only cells that contained a visible nucleus and nucleolus and contacted by at least one VGLUT1-positive puncta and were selected for analysis. Multipolar cells were not divided into subtypes. Most multipolar cells observed were contacted by numerous VGLUT1-positive puncta. We were unable to sample a sufficient number of octopus cells in cross section to perform an analysis. Cross-sectional cell body area, cell body perimeter, and the area of VGLUT1-positive puncta contacting the cell body perimeter were traced in Adobe Photoshop and measured using ImageJ software. The cell body cross-sectional size, number of puncta per 10 microns cell body perimeter, and cross-sectional area of puncta were calculated for 17 bushy cells and 42 multipolar cells in three 1-2 month, and 19 bushy cells and 42 multipolar cells in three 9-10 month DBA/1J mice. Student's t-tests for samples were calculated to identify statistically significant differences.

4.3.5 Transmission electron microscopy (TEM)—Two 2-month old and two 7-8 month old DBA/2J mice were processed for TEM analysis. Sectioning was completed as described above except that sections were cut at a thickness of 75 microns. Sections were

postfixed with osmium tetroxide, stained with uranyl acetate, and flat-embedded in a Polybed 812 solution. Areas from the magnocellular core of the mid to posterior portion of anterior VCN were cut from the plastic-embedded sections and re-embedded in BEEM capsules for ultrathin sectioning (70 nm). Randomly chosen sections were scanned for cell bodies and photographed at a low (3000x) magnification using a Hitachi (H7600) transmission electron microscope. Bushy cells in which a cross section of the cell body, nucleus, and, when possible, the nucleolus were visible were chosen for higher magnification photographs. Axosomatic endbulb profiles containing clear large round synaptic vesicles, glial sheaths, and opposing postsynaptic densities were photographed at high magnification (15,000-30,000x).

Acknowledgments

We thank Mohamed Lehar, Tan Pongstaporn, William Yu, and the Center for Hearing and Balance core for technical assistance and Heather Graham for assistance with figure preparation. Supported by NIH grants DC012352, DC005211, EY001765, and the American Hearing Research Foundation, NHMRC 1009482, and the Oticon Foundation. The content is solely the responsibility of the authors and does not necessarily represent the official views of the funding agencies.

Abbreviations

ABR	auditory brainstem response
ASR	acoustic startle reflex
SPL	sound pressure level
TEM	transmission electron microscopy
VCN	ventral cochlear nucleus
VGLUT1	vesicular glutamate transporter 1

References

Ding, D.; McFadden, SL.; Salvi, RJ. Cochlear hair cell densities and inner ear staining techniques. In: Willott, JF., editor. Handbook of Mouse Auditory Research: From Behavior to Molecular Biology. CRC Press; 2001. p. 189

Erway LC, Willott JF, Archer JR, Harrison DE. Genetics of age-related hearing loss in mice: I. inbred and F1 hybrid strains. Hear Res. 1993; 65:125–132. [PubMed: 8458745]

Furman AC, Kujawa SG, Liberman MC. Noise-induced cochlear neuropathy is selective for fibers with low spontaneous rates. J Neurophysiol. 2013; 110:577–586. [PubMed: 23596328]

Fyk-Kolodziej B, Shimano T, Gong TW, Holt AG. Vesicular glutamate transporters: Spatio-temporal plasticity following hearing loss. Neuroscience. 2011; 178:218–239. [PubMed: 21211553]

Gentschev T, Sotelo C. Degenerative patterns in the ventral cochlear nucleus of the rat after primary deafferentation. an ultra-structural study. Brain Res. 1973; 62:37–60. [PubMed: 4765119]

Gómez-Nieto R, Rubio ME. A bushy cell network in the rat ventral cochlear nucleus. J Comp Neurol. 2009; 516:241–263. [PubMed: 19634178]

Green KM, Bhatt Y, Mawman DJ, O'Driscoll MP, Saeed SR, Ramsden RT, Green MW. Predictors of audiological outcome following cochlear implantation in adults. Cochlear Implants Int. 2007; 8:1–11. [PubMed: 17479968]

Hildebrandt H, Hoffmann NA, Illing RB. Synaptic reorganization in the adult rat's ventral cochlear nucleus following its total sensory deafferentation. PLoS One. 2011; 6:e23686. [PubMed: 21887295]

Ison, JR. The acoustic startle response: Reflex elicitation and reflex modification by preliminary stimuli. In: Willott, JF., editor. The Handbook of Mouse Auditory Research: From Behavior to Molecular Biology. CRC Press; 2001. p. 59

Johnson KR, Longo-Guess C, Gagnon LH, Yu H, Zheng QY. A locus on distal chromosome 11 (ahl8) and its interaction with Cdh23 ahl underlie the early onset, age-related hearing loss of DBA/2J mice. Genomics. 2008; 92:219–225. [PubMed: 18662770]

Kim JJ, Gross J, Potashner SJ, Morest DK. Fine structure of long-term changes in the cochlear nucleus after acoustic overstimulation: Chronic degeneration and new growth of synaptic endings. J Neurosci Res. 2004; 77:817–828. [PubMed: 15334600]

Knipper M, da Penha Berzaghi M, Blochl A, Breer H, Thoenen H, Lindholm D. Positive feedback between acetylcholine and the neurotrophins nerve growth factor and brain-derived neurotrophic factor in the rat hippocampus. Eur J Neurosci. 1994a; 6:668–671. [PubMed: 8025717]

Knipper M, Leung LS, Zhao D, Rylett RJ. Short-term modulation of glutamatergic synapses in adult rat hippocampus by NGF. Neuroreport. 1994b; 5:2433–2436. [PubMed: 7696574]

Kraus KS, Ding D, Jiang H, Lobarinas E, Sun W, Salvi RJ. Relationship between noise-induced hearing-loss, persistent tinnitus and growth-associated protein-43 expression in the rat cochlear nucleus: Does synaptic plasticity in ventral cochlear nucleus suppress tinnitus? Neuroscience. 2011; 194:309–325. [PubMed: 21821100]

Lang H, Schulte BA, Schmiedt RA. Endocochlear potentials and compound action potential recovery: Functions in the C57BL/6J mouse. Hear Res. 2002; 172:118–126. [PubMed: 12361874]

Lauer AM, May BJ. The medial olivocochlear system attenuates the developmental impact of early noise exposure. Journal of the Association for Research in Otolaryngology. 2011; 12:329–343. [PubMed: 21347798]

Lauer AM, Connelly CJ, Graham H, Ryugo DK. Morphological characterization of bushy cells and their inputs in the laboratory mouse (mus musculus) anteroventral cochlear nucleus. PLoS One. 2013; 8:e73308. [PubMed: 23991186]

Lauer AM, Fuchs PA, Ryugo DK, Francis HW. Efferent synapses return to inner hair cells in the aging cochlea. Neurobiol Aging. 2012; 33:2892–2902. [PubMed: 22405044]

Lauer AM, May BJ, Hao ZJ, Watson J. Analysis of environmental sound levels in modern rodent housing rooms. Lab Anim (NY). 2009; 38:154–160. [PubMed: 19384312]

Lazard DS, Bordure P, Lina-Granade G, Magnan J, Meller R, Meyer B, Radafy E, Roux PE, Gnansia D, Pean V, Truy E. Speech perception performance for 100 post-lingually deaf adults fitted with neurelec cochlear implants: Comparison between digisonic(R) convex and digisonic(R) SP devices after a 1-year follow-up. Acta Otolaryngol. 2010; 130:1267–1273. [PubMed: 20446821]

Lee DJ, Cahill HB, Ryugo DK. Effects of congenital deafness in the cochlear nuclei of shaker-2 mice: An ultrastructural analysis of synapse morphology in the endbulbs of held. J Neurocytol. 2003; 32:229–243. [PubMed: 14724386]

Liberman MC, Dodds LW. Single-neuron labeling and chronic cochlear pathology. III. stereocilia damage and alterations of threshold tuning curves. Hear Res. 1984; 16:55–74. [PubMed: 6511673]

Liberman MC, Kiang NY. Acoustic trauma in cats. cochlear pathology and auditory-nerve activity. Acta Otolaryngol Suppl. 1978; 358:1–63. [PubMed: 281107]

Lina IA, Lauer AM. Rapid measurement of auditory filter shape in mice using the auditory brainstem response and notched noise. Hear Res. 2013; 298:73–79. [PubMed: 23347916]

Meidinger MA, Hildebrandt-Schoenfeld H, Illing RB. Cochlear damage induces GAP-43 expression in cholinergic synapses of the cochlear nucleus in the adult rat: A light and electron microscopic study. Eur J Neurosci. 2006; 23:3187–3199. [PubMed: 16820009]

Mikuriya T, Sugahara K, Sugimoto K, Fujimoto M, Takemoto T, Hashimoto M, Hirose Y, Shimogori H, Hayashida N, Inouye S, Nakai A, Yamashita H. Attenuation of progressive hearing loss in a model of age-related hearing loss by a heat shock protein inducer, geranylgeranylacetone. Brain Res. 2008; 1212:9–17. [PubMed: 18445491]

Miller JM, Chi DH, O'Keeffe LJ, Kruszka P, Raphael Y, Altschuler RA. Neurotrophins can enhance spiral ganglion cell survival after inner hair cell loss. Int J Dev Neurosci. 1997; 15:631–643. [PubMed: 9263039]

Mulders W, Rodger J, Albertsen M, Yates C, Robertson D. Effects of cochlear trauma on BDNF expression in guinea pig cochlear nucleus and inferior colliculus. Otolaryngology S3. 2014; 6:2.

Noben-Trauth K, Zheng QY, Johnson KR. Association of cadherin 23 with polygenic inheritance and genetic modification of sensorineural hearing loss. Nat Genet. 2003; 35:21–23. [PubMed: 12910270]

Schettino AE, Lauer AM. The efficiency of design-based stereology in estimating spiral ganglion populations in mice. Hear Res. 2013; 304:153–158. [PubMed: 23876522]

Shin JB, Longo-Guess CM, Gagnon LH, Saylor KW, Dumont RA, Spinelli KJ, Pagana JM, Wilmarth PA, David LL, Gillespie PG, Johnson KR. The R109H variant of fascin-2, a developmentally regulated actin crosslinker in hair-cell stereocilia, underlies early-onset hearing loss of DBA/2J mice. J Neurosci. 2010; 30:9683–9694. [PubMed: 20660251]

Someya S, Yamasoba T, Prolla TA, Tanokura M. Genes encoding mitochondrial respiratory chain components are profoundly down-regulated with aging in the cochlea of DBA/2J mice. Brain Res. 2007; 1182:26–33. [PubMed: 17964557]

Suneja SK, Yan L, Potashner SJ. Regulation of NT-3 and BDNF levels in guinea pig auditory brain stem nuclei after unilateral cochlear ablation. J Neurosci Res. 2005; 80:381–390. [PubMed: 15795930]

Taberner AM, Liberman MC. Response properties of single auditory nerve fibers in the mouse. J Neurophysiol. 2005; 93:557–569. [PubMed: 15456804]

Turner JG, Willott JF. Exposure to an augmented acoustic environment alters auditory function in hearing-impaired DBA/2J mice. Hear Res. 1998; 118:101–113. [PubMed: 9606065]

Wang Y, Manis PB. Temporal coding by cochlear nucleus bushy cells in DBA/2J mice with early onset hearing loss. J Assoc Res Otolaryngol. 2006; 7:412–424. [PubMed: 17066341]

Wang Y, Manis PB. Synaptic transmission at the cochlear nucleus endbulb synapse during age-related hearing loss in mice. J Neurophysiol. 2005; 94:1814–1824. [PubMed: 15901757]

Willott JF, Bross LS, McFadden S. Ameliorative effects of exposing DBA/2J mice to an augmented acoustic environment on histological changes in the cochlea and anteroventral cochlear nucleus. J Assoc Res Otolaryngol. 2005; 6:234–243. [PubMed: 15983726]

Willott JF, Erway LC. Genetics of age-related hearing loss in mice. IV. cochlear pathology and hearing loss in 25 BXD recombinant inbred mouse strains. Hear Res. 1998; 119:27–36. [PubMed: 9641316]

Willott JF. Comparison of response properties of inferior colliculus neurons of two inbred mouse strains differing in susceptibility to audiogenic seizures. J Neurophysiol. 1981; 45:35–47. [PubMed: 7205343]

Xie R, Manis PB. Glycinergic synaptic transmission in the cochlear nucleus of mice with normal hearing and age-related hearing loss. J Neurophysiol. 2013; 110:1848–1859. [PubMed: 23904491]

Yuan Y, Shi F, Yin Y, Tong M, Lang H, Polley DB, Liberman MC, Edge AS. Ouabain-induced cochlear nerve degeneration: Synaptic loss and plasticity in a mouse model of auditory neuropathy. Journal of the Association for Research in Otolaryngology. 2014; 15:31–43. [PubMed: 24113829]

Zeng C, Nannapaneni N, Zhou J, Hughes LF, Shore S. Cochlear damage changes the distribution of vesicular glutamate transporters associated with auditory and nonauditory inputs to the cochlear nucleus. J Neurosci. 2009a; 29:4210–4217. [PubMed: 19339615]

Zeng C, Nannapaneni N, Zhou J, Hughes LF, Shore S. Cochlear damage changes the distribution of vesicular glutamate transporters associated with auditory and nonauditory inputs to the cochlear nucleus. J Neurosci. 2009b; 29:4210–4217. [PubMed: 19339615]

Highlights

- Central auditory nerve synapses was evaluated mice with early-onset deafness
- Number of auditory nerve synapses was similar in deaf mice and hearing mice
- Auditory nerve terminals were smaller in deaf mice compared to hearing mice

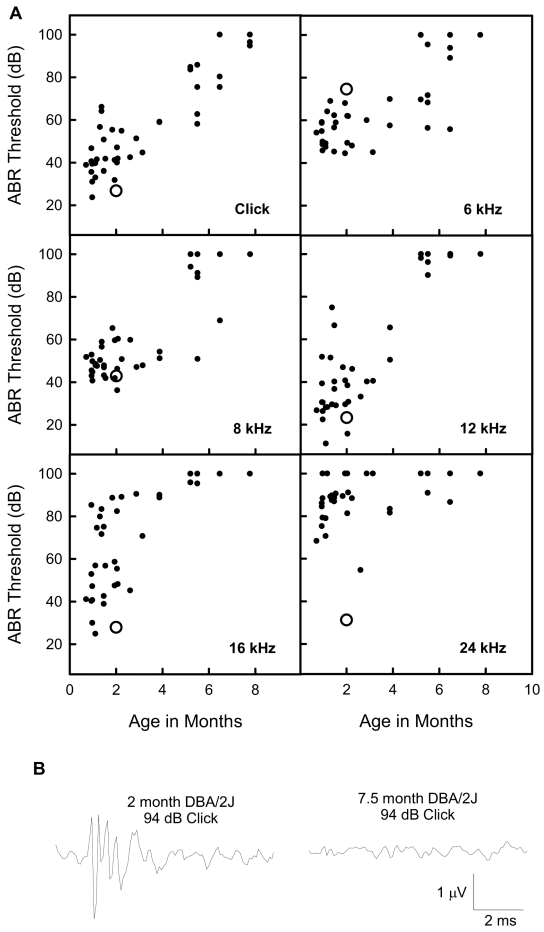

Figure 1.

Auditory brainstem responses (ABR) thresholds for DBA/2J mice as a function of age. A) individual DBA/2J mice (filled circles) and average CBA/CaJ thresholds at 2 months of age (large open circles). DBA/2J mice show a profound hearing loss by 5 months of age. Click thresholds are in dB peak equivalent level. Tone thresholds are in dB sound pressure level (SPL). B) Examples of ABR waveforms from a young, hearing DBA/2J and an older, deaf DBA/2J mouse evoked by broadband clicks.

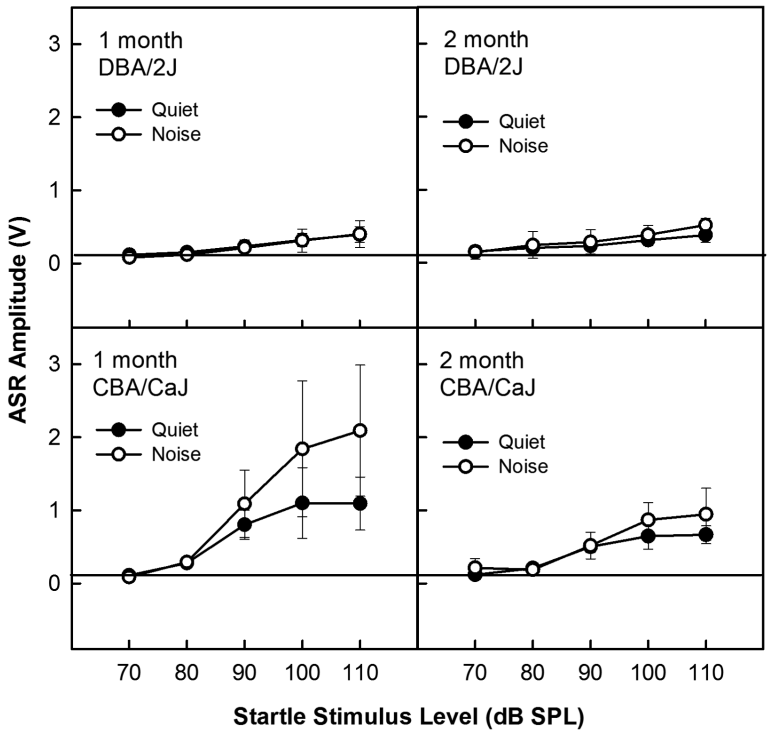

Figure 2.

Acoustic startle responses (ASR) to short bursts of broadband noise presented in quiet or continuous 60 dB SPL broadband noise in 1 and 2 month old DBA/2J (A, B) and CBA/CaJ (C, D) mice. The horizontal line near zero indicates the level of background activity when the mouse is at rest. Error bars indicate standard deviation.

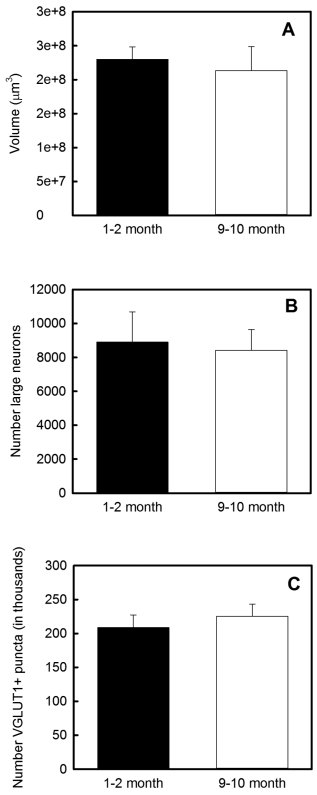

Figure. 3.

Stereological analysis of VCN. Ventral cochlear nucleus (VCN) volume (A), large cell number (B), and number of VLGUT1-positive auditory nerve puncta (C) are similar in young hearing and older deaf DBA/2J mice. Error bars indicate standard deviation.

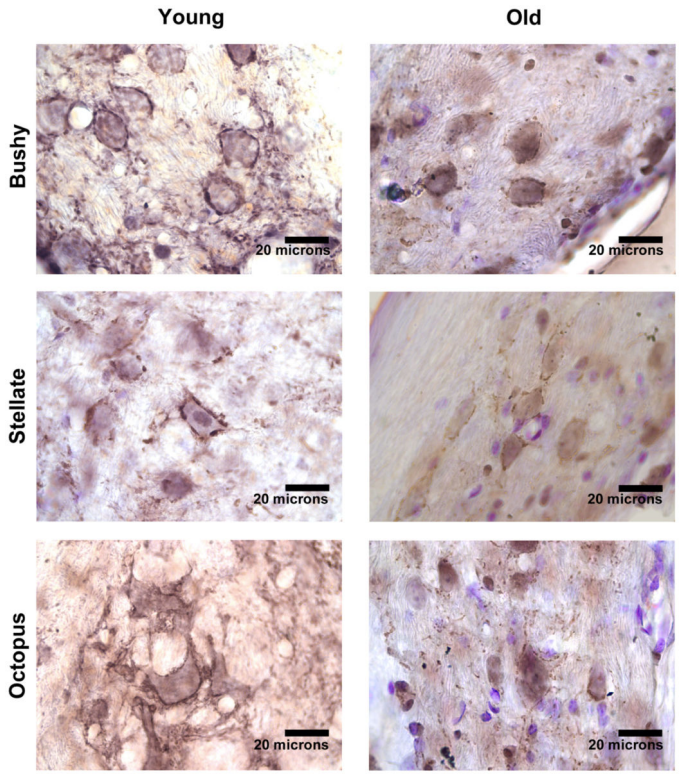

Figure 4.

VGLUT1 immunolabeling in DBA/2J mouse VCN. Numerous VGLUT1-positive terminals in hearing and deaf DBA/2J mice contact VCN bushy, multipolar, and octopus cells.

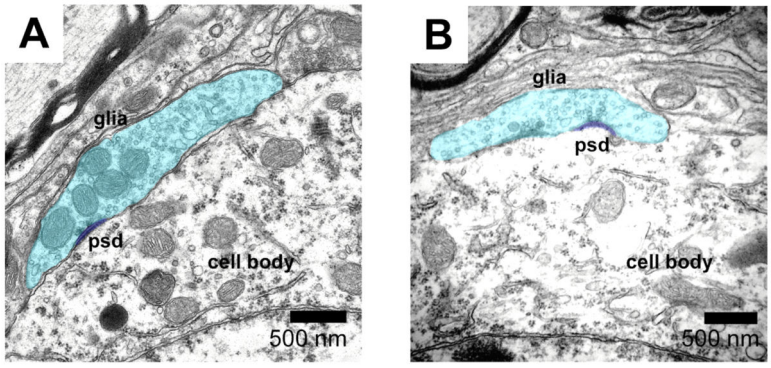

Figure 5.

Transmission electron micrographs reveal ultrastructural details of auditory nerve synapses in DBA/2J mice. A) Profiles of axosomatic endbulb synapses appear normal in young hearing DBA/2J mice, displaying short, curved postsynaptic densities (psd), numerous clear large round synaptic vesicles, and glial sheaths (glia). B) Axosomatic endbulb synapse profiles appeared similar, but smaller in deaf DBA/2J mice.

Table 1

Means and standard deviations for VCN cell body and VGLUT1-positive puncta measurements in 1-2 month and 9-10 month DBA/1J mice.

	Bushy Cells		Multipolar Cells	
	1-2 month	**9-10 month**	**1-2 month**	**9-10 month**
Cell body area (μm^2)	160.0 (47.07)	150.12 (40.52)	140.48 (43.88)	125.97 (39.29)
Number of puncta per 10 μm cell body perimeter	2.56 (0.77)	2.41 (0.88)	2.53 (0.86)	2.67 (1.24)
Puncta area (μm^2)	1.90 (2.09)	1.14 (1.32)	2.01 (2.13)	1.13 (1.43)